
Effect of Size, Shape and Environment on the Optical Response of Metallic Nanoparticles

Salem Marhaba

Additional information is available at the end of the chapter

<http://dx.doi.org/10.5772/intechopen.71574>

Abstract

The aim of this chapter is to investigate the effect of size, shape and environment on the optical properties of metallic nanoparticles in a large spectral range ($\lambda = 300\text{--}900\text{ nm}$) using quasi-static approximation for nanoparticles of sizes ($D = 10\text{--}40\text{ nm}$) and Mie theory for nanoparticles of sizes ($D = 40\text{--}100\text{ nm}$). Extinction (scattering and absorption) cross-sectional spectrum of nanoparticles is obtained for different diameters embedded in different matrices. Collective oscillation of electrons in conduction band in metallic nanoparticles is known as surface plasmon resonance (SPR) phenomena. SPR of metallic nanoparticles has significant applications in optics, communications and biosensors. We present in this chapter the effects of the interparticle distance on the optical response of gold dimer nanoparticles of 100 nm diameter. The extinction spectra of dimer nanoparticles are calculated by using generalized Mie theory.

Keywords: metallic nanoparticles, noble metals, optical properties, surface plasmon resonance, extinction cross section, morphology, dimer of nanoparticles

1. Introduction

Nanomaterials are macroscopic systems but constructed and organized from elementary bricks of nanometric dimensions known as nanoparticles. They have many fields of application, in the fields of optics [1, 2], magnetism [3, 4], electronics [5, 6], telecommunications [7, 8], superconductors [9, 10], chemical catalysis [11] or biological marking [12].

The phenomena of absorption, scattering and reemission of an electromagnetic wave by particles of micrometric or even nanometric size are numerous and varied. For example, sunlight incident on the Earth's atmosphere is dispersed by gas molecules and suspended particles (aerosols), giving rise to a blue sky, white clouds and various optical phenomena such as the rainbows or the halos. Another example that concerns us more closely is that of the

variety of colors of stained-glass windows whose origin is based on the very specific scattering properties of light by very fine metallic grains trapped in transparent glasses [13].

The metallic clusters of nanometric size, well below the optical wavelength, have been known and exploited for centuries for their spectacular optical properties (stained glass, ceramics) [14]. Take, for example, the case of gold nanoparticles, which can be obtained in colloidal form by chemical synthesis. When diluted in solution, they exhibit varying colors, ranging from red to violet as their size decreases. Other colors like green and blue can be obtained by also playing on their shape. These optical properties are a consequence of the dielectric confinement in these objects whose size is less than the wavelength of the excitatory light and which is at the origin of the well-known phenomenon of surface plasmon resonance (SPR), which dominates the extinction spectrum in the visible domain. This oscillation is analogous to that of an electron gas in a massive system (plasmon mode) but modified by the presence of interfaces.

Among the nanoscale systems that possess very interesting optical properties, metals and especially noble metals (gold, silver and copper) have been the most widely studied in this way [15–17]. Noble metals and gold in particular lend themselves well to the synthesis of such materials, thanks to their resistance to aging (oxidation), even in a divided form. Great progress has been made in understanding the optical properties of composite materials based on nanoparticle well as in their methods of synthesis. These range from techniques of precipitation of metal salts in glasses or gels, to the assembly of preformed particles, chemically (colloid) or physically (sources of clusters).

In this chapter, we recall the theoretical results concerning the optical properties of bulk and confined metal systems. Particular emphasis is placed on the remarkable origin and properties of surface plasmon resonance (SPR) and its dependence on the size, shape and dielectric environment of nanoparticles. We study the basic formalisms for the calculation of the different cross sections of nanoparticle interaction with light (extinction, scattering and absorption) in the framework of:

- i. Quasi-static approximation for spherical and spheroidal particles
- ii. Mie theory for homogeneous spherical particles.

Finally, we briefly discuss the effects of the interparticle distance on the optical response of dimer nanoparticles based on the generalized Mie theory.

2. Drude model and plasma frequency

The first situation envisaged, since it is the simplest, is that of a metal whose optical properties are essentially due to the behavior of the conduction electrons (as for the alkali metals). The Drude model [18] is then quite appropriate to describe the behavior of these quasi-free electrons. In this model, the conduction electrons of solid metal, considered as independent, move almost freely. These electrons undergo random collisions with other particles (other electrons, phonons, defects, etc.), with a probability per unit of time given by the electronic collision

(or relaxation) rate $\gamma_0 = \tau^{-1}$. The corresponding time τ is connected to the mean free path of the electrons by $l = v_F \tau$ where v_F is the Fermi velocity of conduction electrons. For example, in the case of bulk sodium, $l \cong 35$ nm at 273 K [4] and $v_F = 1.07$ nm.fs⁻¹ [19], resulting an average collision time $\tau \cong 32$ fs (estimated from electrical resistivity measurements [20]). Each collision is an instantaneous event with a sudden change in the speed of the electron, without memory of its initial velocity. The average effect of these collisions, which the Drude model does not claim to describe the mechanism, can then be modeled by a friction force whose damping coefficient is γ_0 . In the presence of an external field $\vec{E} = \vec{E}_0 e^{-i\omega t}$, the fundamental principle of the dynamics applied to a conduction electron of effective mass m_{eff} and of charge $-e$ is written as:

$$m_{eff} \frac{d^2 \vec{r}}{dt^2} = -\frac{m_{eff}}{\tau} \frac{d\vec{r}}{dt} - e\vec{E} \quad (1)$$

In this equation, \vec{r} is the displacement of the electron around an average position, and the second term is a damping term related to the different collision processes cited above. An oscillating solution of this equation is as follows:

$$\vec{r} = \frac{e\vec{E}}{m_e \omega (\omega + i\gamma_0)} \quad (2)$$

The displacement of Drude's electrons induces a dipole moment $\vec{p} = -e\vec{r}$, and the electron gas polarization, defined as the dipolar moment per unit volume, is thus written as:

$$\vec{P} = -ne\vec{r} = \frac{-\epsilon_0 \omega_p^2}{\omega^2 + i\gamma_0 \omega} \vec{E} \quad (3)$$

where n is the number of free electrons per unit volume and $\omega_p = \sqrt{\frac{ne^2}{m_e \epsilon_0}}$ is called plasma frequency of bulk metal. The Drude model allows us to introduce simply the notion of dielectric constant, a characteristic magnitude of the optical response of a solid.

3. Dielectric constant and dielectric susceptibility

In a material, the two macroscopic vector quantities, which are the electric field \vec{E} and the electric displacement \vec{D} , are connected together by the relation

$$\vec{D} = \epsilon_0 \vec{E} + \vec{P} \quad (4)$$

where ϵ_0 is the vacuum permittivity and \vec{P} is the induced electrical polarization. Since the intensity of the applied field is not too high, the polarization \vec{P} is connected linearly with \vec{E} through the dielectric susceptibility χ of the medium according to the relation:

$$\vec{P} = \epsilon_0 \chi \vec{E} \quad (5)$$

which allows us to establish a relation between the electric displacement and the electric field by defining the dielectric constant ϵ such that:

$$\vec{D} = \epsilon_0 \epsilon \vec{E} \text{ with } \epsilon = 1 + \chi \quad (6)$$

By combining the three equations: Eqs. (3), (4) and (6), the dielectric constant ϵ is obtained in the form:

$$\epsilon(\omega) = 1 - \frac{\omega_p^2}{\omega(\omega + i\gamma_0)} \quad (7)$$

The dielectric constant $\epsilon(\omega)$ is generally written in complex form:

$$\epsilon(\omega) = \epsilon_1(\omega) + i\epsilon_2(\omega) \quad (8)$$

The real and imaginary parts of $\epsilon(\omega)$ are written as:

$$\begin{cases} \epsilon_1(\omega) = 1 - \frac{\omega_p^2}{\omega^2 + \gamma_0^2} \\ \epsilon_2(\omega) = \frac{\omega_p^2 \gamma_0}{\omega(\omega^2 + \gamma_0^2)} \end{cases} \quad (9)$$

In the optical domain where the frequencies are such that $\omega \gg \gamma_0$, these expressions are simplified in the form:

$$\begin{cases} \epsilon_1(\omega) = 1 - \frac{\omega_p^2}{\omega^2} \\ \epsilon_2(\omega) = \frac{\omega_p^2}{\omega^3} \gamma_0 \end{cases} \quad (10)$$

We then see, in a classical approach, how the core electrons are introduced in the study of the optical properties of noble metals.

4. Interband absorption: contribution of d electrons

The optical response of bulk noble metals cannot be completely described by the Drude model. To take into account the contribution of core electrons (d band electrons) in the optical response of noble metals, a term must be added to the dielectric constant as calculated from the Drude model (Eq. 9). The dielectric constant can be written in the following way:

$$\epsilon = 1 + \chi^D + \chi^{IB} \text{ or } \epsilon = \epsilon^D + \epsilon^{IB} - 1; \tag{11}$$

ϵ^D and ϵ^{IB} are complex ($\epsilon^D = 1 + \chi^D$ and $\epsilon^{IB} = 1 + \chi^{IB}$).

The first term ϵ^D represents the intraband component of the dielectric constant. It is connected to the optical transitions of a free electron of the conduction band to a higher energy level of the same band. This term is well described by the Drude model, hence the index D . The second term ϵ^{IB} corresponds to the interband component of the dielectric constant, linked to the optical transitions between the valence band (essentially from the d band) and the conduction band sp. There is, therefore, a threshold energy E^{IB} for interband transitions (located in the visible (for gold) or near UV (for silver)). This component may be neglected in the infrared domain, where the optical response is dominated by intraband absorption. The real and imaginary parts of the experimental dielectric constants of gold and silver, as given in Johnson and Christy [21] and Palik [22], represented in **Figures 1** and **2**, reproduce well the predictions of the Drude model (Eq. 9) in the sense that they diverge very similarly for low energies ($E < 1.5$ eV approximately).

The role of the core electrons d is manifested by the deviation from the Drude function. It is mainly observed in the imaginary parts of ϵ . The strong growth of the imaginary component ϵ_2 , observed around 620 nm for gold and 310 nm for silver, marks the beginning of interband transitions. It should be noted that the dielectric constants tabulated in the literature may differ according to the sources since they are extracted from experimental measurements obtained with techniques and under conditions which may be different. For example, some discrepancies between the values of Palik and those of Johnson and Christy may have important implications for the predictions of theoretical models when injected into calculations.

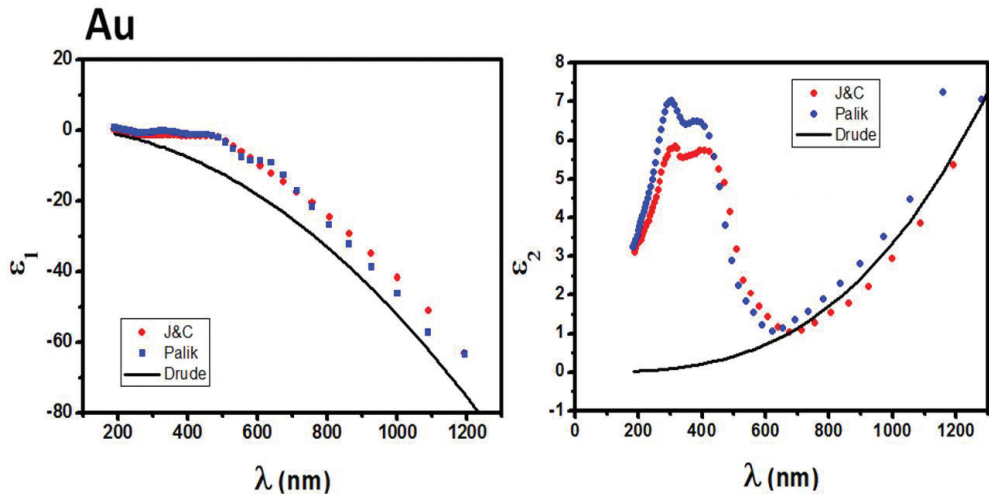


Figure 1. Real and imaginary parts of the dielectric constant of bulk gold. The experimental results of Johnson and Christy (red •) and Palik (blue •) are compared to the Drude model (solid lines).

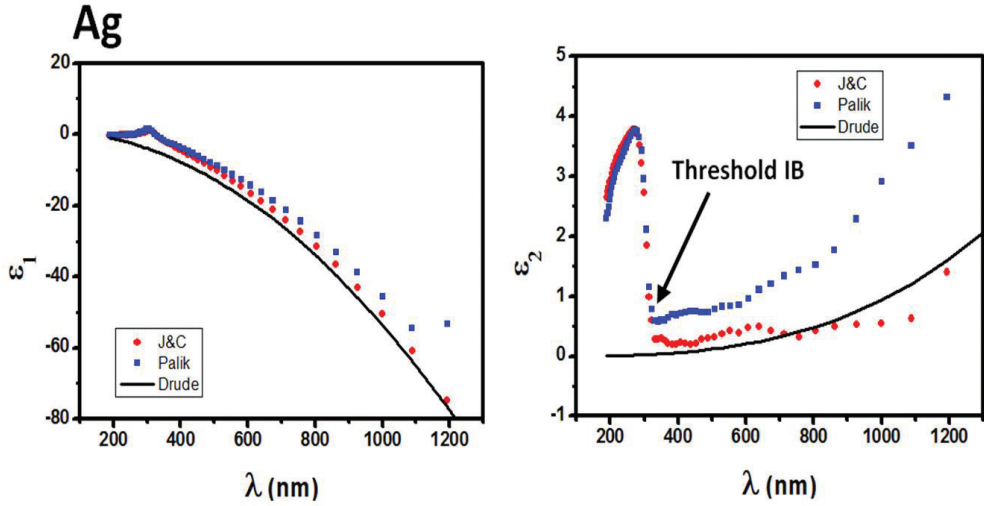


Figure 2. Real and imaginary parts of the dielectric constant of bulk silver. The experimental results of Johnson and Christy (red •) and Palik (blue •) are compared to the Drude model (solid lines).

5. Extinction, scattering and absorption of wave by a sphere in the quasi-static approximation

We study the optical response of a metal sphere in the quasi-static approximation, that is to say when the wavelength λ of the incident radiation (plane wave) is much greater than the diameter D of the sphere. In this case, it is possible to consider that the applied electromagnetic field is uniform at each instant and at any point of the object volume (no delay effect). The sphere of radius R is characterized by a complex dielectric constant. The dielectric constant ϵ_m of the environment is real since this dielectric medium is transparent in our frequency domain ($n_m = \sqrt{\epsilon_m}$). In the quasi-static approximation and if the temporal variation of the applied field is set aside, the problem returns to that of a sphere subjected to a uniform field \vec{E}_0 . The electric potentials take the form [23]:

$$\begin{cases} V_1(r, \theta) = -\frac{3\epsilon_m}{\epsilon_1 + 2\epsilon_m} E_0 r \cos \theta \\ V_m(r, \theta) = -E_0 r \cos \theta + R^3 E_0 \frac{\epsilon_1 - \epsilon_m}{\epsilon_1 + 2\epsilon_m} \frac{\cos \theta}{r^2} = V_i(r, \theta) + V_s(r, \theta) \end{cases} \quad (12)$$

V_i is the electric potential due to the incident electric field E_0 , and V_s is the electric potential due to the scattered electric field E_s .

Given the symmetry of the problem, the azimuthal angular dependence ϕ does not intervene, and then the system is reduced to a two-dimensional problem: r and θ . The internal field is uniform $\vec{E}_1 = -\vec{\nabla} V_1 = \frac{3\epsilon_m}{\epsilon_1 + 2\epsilon_m} \vec{E}_0$, and from the expression of V_m above, we see that the total

external field is the sum of the incident field derived from V_i and an additional field \vec{E}_s derived from V_s . Note that V_s has the structure of the potential generated by a dipole:

$$V_s(r, \theta) = R^3 E_0 \frac{\epsilon_1 - \epsilon_m}{\epsilon_1 + 2\epsilon_m} \frac{\cos \theta}{r^2} = \frac{\vec{p} \cdot \vec{r}}{4\pi\epsilon_m r^3} \quad (13)$$

where \vec{p} is written as

$$\vec{p} = 4\pi\epsilon_m R^3 \frac{\epsilon_1 - \epsilon_m}{\epsilon_1 + 2\epsilon_m} \vec{E}_0 \quad (14)$$

The application of the electric field \vec{E}_0 induces a polarization of the sphere (**Figure 3**) and the appearance of a charge surface distribution:

$$\sigma(\theta) = 3 \frac{\epsilon_1 - \epsilon_m}{\epsilon_1 + 2\epsilon_m} E_0 \cos \theta \quad (15)$$

One can write: $\vec{p} = 3\epsilon_m \alpha \vec{E}_0$

where

$$\alpha = V \frac{\epsilon_1 - \epsilon_m}{\epsilon_1 + 2\epsilon_m} \quad (16)$$

α is defined as the polarizability of the sphere, and $V = 4/3\pi R^3$ is the volume of the particle. The extinction and scattering cross sections in general form are

$$C_{ext} = 3k \operatorname{Im}\{\alpha\} = 3kV \operatorname{Im}\left\{ \frac{\epsilon_1 - \epsilon_m}{\epsilon_1 + 2\epsilon_m} \right\} \quad (17)$$

$$C_{diff} = \frac{3k^4}{2\pi} |\alpha|^2 = \frac{3}{2} k^4 V^2 \left| \frac{\epsilon_1 - \epsilon_m}{\epsilon_1 + 2\epsilon_m} \right|^2 \quad (18)$$

$$C_{abs} = C_{ext} - C_{diff} \quad (19)$$

The essential point here is that the polarization and consequently the different cross sections can become very important if the common term to their denominator vanishes or takes very low values. Knowing that the dielectric constant ϵ_1 of the metal (Eq. 5) depends on the frequency of the excitation wave, a resonance phenomenon is observed when

$$|\epsilon_1 + 2\epsilon_m|^2 = [\operatorname{Re}\{\epsilon_1(\omega)\} + 2\epsilon_m]^2 + \operatorname{Im}\{\epsilon_1(\omega)\}^2 \quad (20)$$

will be minimum.

If the imaginary component $\operatorname{Im}\{\epsilon_1(\omega)\} \ll 1$ or its variation $\partial \operatorname{Im}\{\epsilon_1(\omega)\} / \partial \omega$ is minimal, then the expression (Eq. 20) can cancel out for a pulsation $\omega = \omega_{RPS}$ such as $\operatorname{Re}\{\epsilon_1(\omega_{RPS})\} = -2\epsilon_m$. By writing the dielectric constant of the determined metal in the case of noble metals (Eq. 8)

and using the Drude model to explain the contribution of free electrons (Eq. 7), we deduce the expression of resonance pulsation ω_{RPS} :

$$\omega_{RPS} = \frac{\omega_p}{\sqrt{\text{Re}\{\epsilon^{(IB)}(\omega_{RPS})\} + 2\epsilon_m}} \tag{21}$$

In the dipolar approximation, the pulsation ω_{RPS} is conventionally interpreted as the oscillation pulsation of the electronic cloud with respect to the ions of the nanoparticle. Such a phenomenon is associated with a collective excitation of electrons within the metallic nanoparticles and known as surface plasmon resonance due to the fact that the restoring force which intervenes in the oscillatory motion is mainly due to the charges located at the surface as this is illustrated in **Figure 3** [24]. By explicating the real and imaginary parts of the dielectric constant of the metal and the wave vector k , the extinction and scattering cross sections (Eqs. 17 and 18) can be written as:

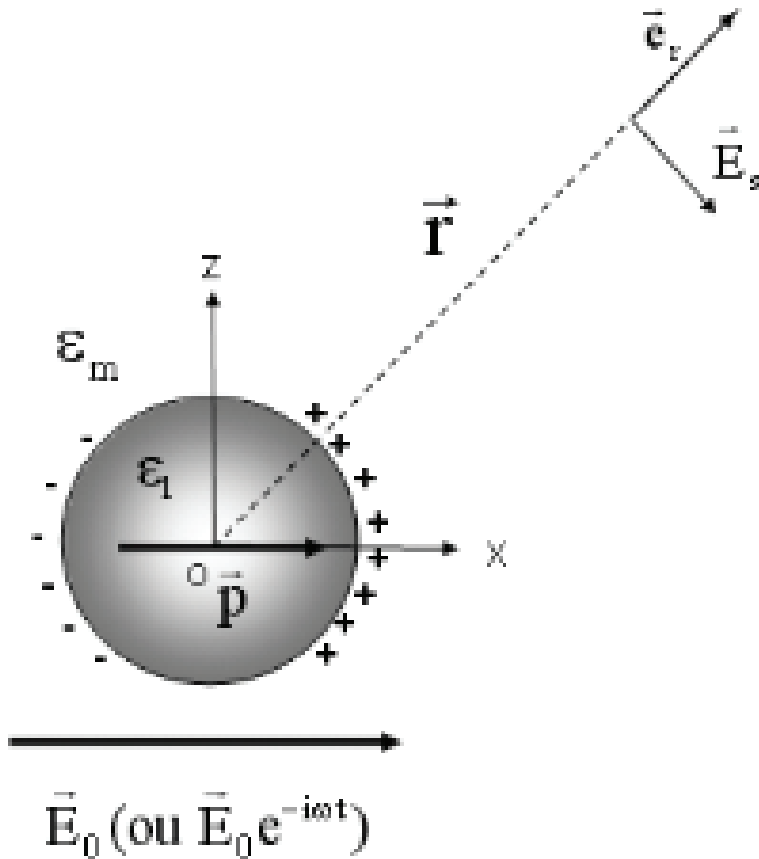


Figure 3. Polarization of a sphere metal subjected to a uniform field E_0 . The dipole radiates a field E_s .

$$\sigma_{ext}(\lambda) = 18\pi\epsilon_m^{3/2} \frac{V}{\lambda} \frac{\epsilon_I(\lambda)}{(\epsilon_R(\lambda) + 2\epsilon_m)^2 + (\epsilon_I(\lambda))^2} \quad (22)$$

$$\sigma_{diff}(\lambda) = 144\pi^4 \epsilon_m^2 \left(\frac{V^2}{\lambda^4}\right) \frac{(\epsilon_R(\lambda) - \epsilon_m)^2 + (\epsilon_I(\lambda))^2}{(\epsilon_R(\lambda) + 2\epsilon_m)^2 + (\epsilon_I(\lambda))^2} \quad (23)$$

Here, $\epsilon_R = \text{Re}\{\epsilon\}$ and $\epsilon_I = \text{Im}\{\epsilon\}$ and we note C_{ext} and C_{scat} in the more usual form σ_{ext} and σ_{scat} . It is chosen to express the spectral dependence of these quantities as a function of the wavelength. We find the dependence in $1/\lambda^4$ of σ_{scat} , characteristic of Rayleigh scattering of nanometric particles. For the same nanoparticle, the ratio of the scattering and extinction cross sections is proportional to the volume V :

$$\frac{\sigma_{diff}}{\sigma_{ext}} \propto \frac{V}{\lambda^3} \propto \left(\frac{R}{\lambda}\right)^3 \quad (24)$$

Thus, for nanoparticles such as $R < \lambda$, that is, in the quasi-static approximation considered so far, extinction is largely dominated by absorption and we have:

$$\sigma_{abs} \cong \sigma_{ext} \quad (25)$$

6. Dielectric constant of a confined system

In the previous description, the dielectric constant of the particles was taken as that of solid bulks. This explains, for example, the absence of size effects on the value of the SPR in the quasi-static approximation. Strictly speaking, it is expected that the effective dielectric constant of the particles will be different from that of the solid bulk, essentially due to the fact that the confinement and the presence of an interface with the external environment must introduce significant modifications. The confinement can be taken into account in the Drude model by introducing phenomenologically a collision effective term for free electrons with surfaces. When the particle size is smaller than the mean free path of electrons, the collision frequency with the surfaces of a sphere of radius R is proportional to ν/R , where ν is the velocity of the electron. Only the electrons close to the Fermi level can contribute to these collisions (because of Pauli's exclusion principle). The speed ν can therefore be taken equal to the Fermi speed ν_F :

$$\nu_F = \sqrt{\frac{2E_F}{m_{eff}}} \quad (26)$$

The total collision rate is written as [25]

$$\gamma(R) = \gamma_0 + g \frac{\nu_F}{R} \quad (27)$$

where γ_0 is the rate of intrinsic electronic collisions (electron/electron and electron/phonon) of the infinite solid, and the parameter g is a dimensionless corrective factor called a surface scattering coefficient. Its value can be estimated according to the simple quantum-box model.

It is of the order of one [25]. Typically, the collision characteristic times $\frac{1}{\gamma_0}$ are of the order of a few tens of femtoseconds (40 fs for Ag and 30 fs for Au from [20]). It is then assumed that the intraband contribution is given by an expression of Drude model with a collision rate given by Eq. (27). The Drude contribution (Eq. 9) damped is thus written as:

$$\begin{cases} \varepsilon_1^D(\omega, R) = 1 - \frac{\omega_p^2}{\omega^2 + \gamma^2(R)} \\ \varepsilon_2^D(\omega, R) = \frac{\omega_p^2 \gamma(R)}{\omega(\omega^2 + \gamma^2(R))} \end{cases} \quad (28)$$

The dielectric constant of the bulk solid is written as:

$$\varepsilon(\omega, \infty) = \underbrace{\varepsilon^D(\omega, \infty)}_{\text{Drude Massif}} + \varepsilon^{IB}(\omega, \infty) - 1 \quad (29)$$

and the dielectric constant of a confined metal:

$$\varepsilon(\omega, R) = \underbrace{\varepsilon^D(\omega, R)}_{\text{Drude Amortie}} + \varepsilon^{IB}(\omega, R) - 1 \quad (30)$$

The interband transitions are little modified for sizes up to 3 nm [26] and then $\varepsilon^{IB}(\omega, R) \approx \varepsilon^{IB}(\omega, \infty)$; it is therefore possible to obtain the expression of the dielectric constant of a confined metal from Eq. (28) and a knowledge of $\varepsilon^{IB}(\omega, \infty)$. $\varepsilon^{IB}(\omega, R)$ can be estimated by subtracting from the experimental dielectric constant (table) [21, 22] the Drude bulk part (Eq. 9):

$$\varepsilon(\omega, R) \cong \varepsilon^D(\omega, R) + (\varepsilon_{\text{exp}}(\omega, \infty) - \varepsilon^D(\omega, \infty)) \quad (31)$$

$$\varepsilon(\omega, R) \cong \varepsilon_{\text{exp}}(\omega, \infty) + \omega_p^2 \left(\frac{1}{\omega^2 + \gamma_0^2} - \frac{1}{\omega^2 + \gamma^2(R)} \right) + i \frac{\omega_p^2}{\omega} \left(\frac{\gamma(R)}{\omega^2 + \gamma^2(R)} - \frac{\gamma_0}{\omega^2 + \gamma_0^2} \right) \quad (32)$$

In the optical domain, the frequencies are such that $\omega \gg \gamma(R)$ and γ_0 ; the expression of the dielectric constant of confined metal is reduced to:

$$\varepsilon(\omega, R) \approx \varepsilon_{\text{exp}}(\omega, \infty) + i \frac{(\omega_p)^2}{(\omega)^3} \left(g \frac{v_F}{R} \right) \quad (33)$$

The constant g is of the order of unity. Its value and its dependence in R are one of the stakes of the optical studies on the nanoparticles. The reducing size is therefore the main effect of widening and attenuating the surface plasmon resonance band. **Figures 4** and **5** show the calculations of the extinction cross section for 20 nm gold and silver spheres immersed in vacuum by using a modified dielectric constant to take account of confinement effect.

It should be noted that the profile of the spectra is given by Eq. (22) in which the modified value of the dielectric constant of the particle (Eq. 31) is introduced. In the case where the

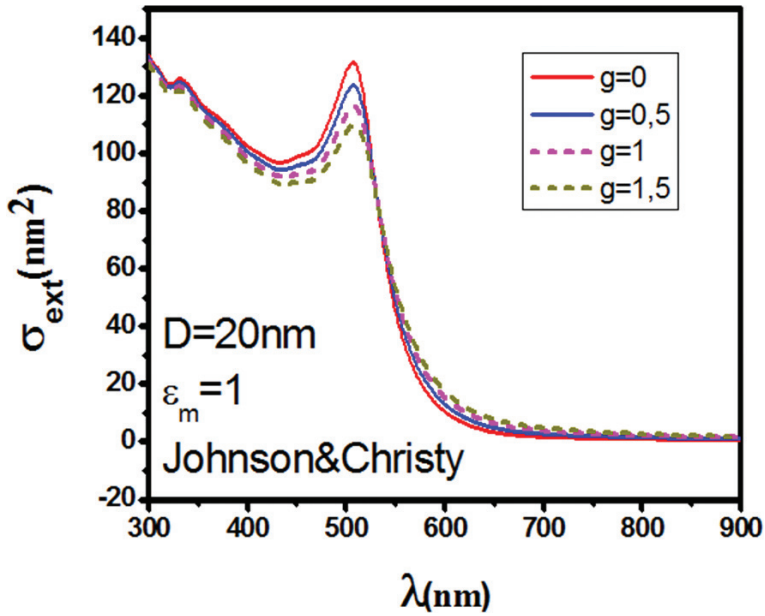


Figure 4. Calculations of the extinction cross sections in the dipolar approximation for a gold nanoparticle with a diameter of 20 nm in a dielectric matrix $\epsilon_m = 1$ for four values of the surface scattering coefficient $g = 0, 0.5, 1$ and 1.5 .

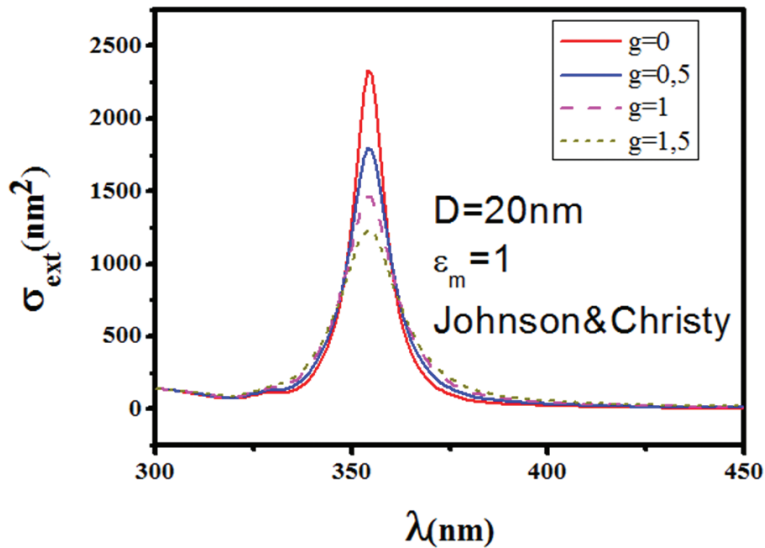


Figure 5. Calculations of the extinction cross sections in the dipolar approximation for a silver nanoparticle with a diameter of 20 nm in a dielectric matrix $\epsilon_m = 1$ for four values of the surface scattering coefficient $g = 0, 0.5, 1$ and 1.5 .

surface plasmon resonance is far from the interband threshold (like silver), it is possible to show that the spectrum adopts a quasi-Lorentzian profile. The full width at half maximum (FWHM) can be expressed approximately in the form [27, 28]:

$$\Gamma \cong \gamma_0 + g \frac{v_F}{R} + \left(\frac{\omega_{RPS}^3}{\omega_p^2} \right) \epsilon_I^{IB}(\omega_{RPS}) = \gamma(R) + \left(\frac{\omega_{RPS}^3}{\omega_p^2} \right) \epsilon_I^{IB}(\omega_{RPS}) \quad (34)$$

The width of the resonance spectrum depends not only on the modified electronic collision rate but also on the imaginary part of the interband dielectric constant in the vicinity of the plasmon resonance. For silver with $g = 1$ and $R = 10$ nm, it is estimated that $\gamma_0 \cong 2.5 \times 10^{13} \text{ s}^{-1}$ ($\tau = 40$ fs) and $g \frac{v_F}{R} \cong 1.4 \times 10^{14} \text{ s}^{-1}$. These two terms contribute to a spectral width $\Delta\lambda \cong 7$ nm around 400 nm. This is consistent with **Figure 5** and indicates that the third term of Eq. (34) contributes little for silver as expected. In this case, an increase in g is sensitive to the width of the spectrum. In the case of gold (**Figure 4**), assuming that Eq. (34) remains fairly valid, one could show that the proximity of the interband transitions with plasmon resonance contributes strongly to the width, which also explains why it is less sensitive to the value of g than in the case of silver.

7. Environment effect on the surface plasmon resonance

From the expression (Eq. 22), it is clear that the extinction cross-sectional spectrum is very sensitive to the value of ϵ_m . For a given metal, the SPR profile can be modified by its environment by means of its dielectric constant ϵ_m . The spectral position will move to red by increasing ϵ_m (Eq. 21). The

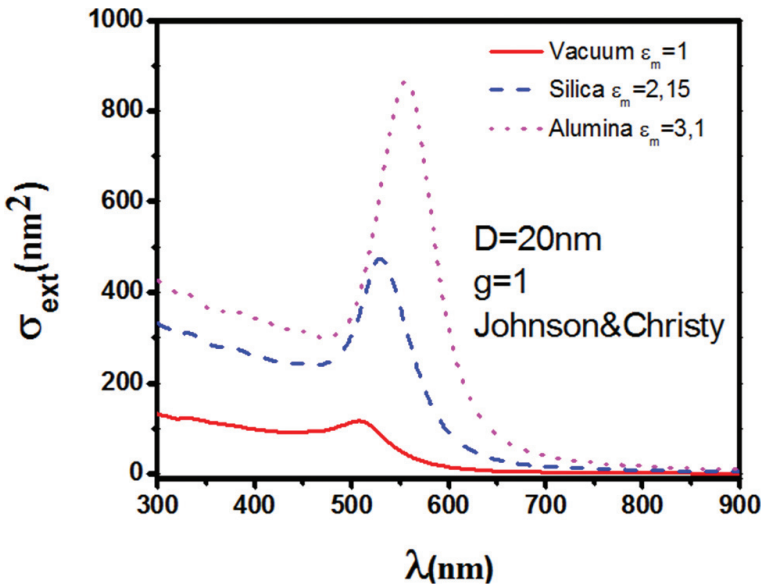


Figure 6. Extinction cross sections for a gold nanoparticle with a diameter of 20 nm calculated by the quasi-static approximation in different environments: Vacuum ($\epsilon_m = 1$), silica ($\epsilon_m = 2, 15$) and alumina ($\epsilon_m = 3, 1$).

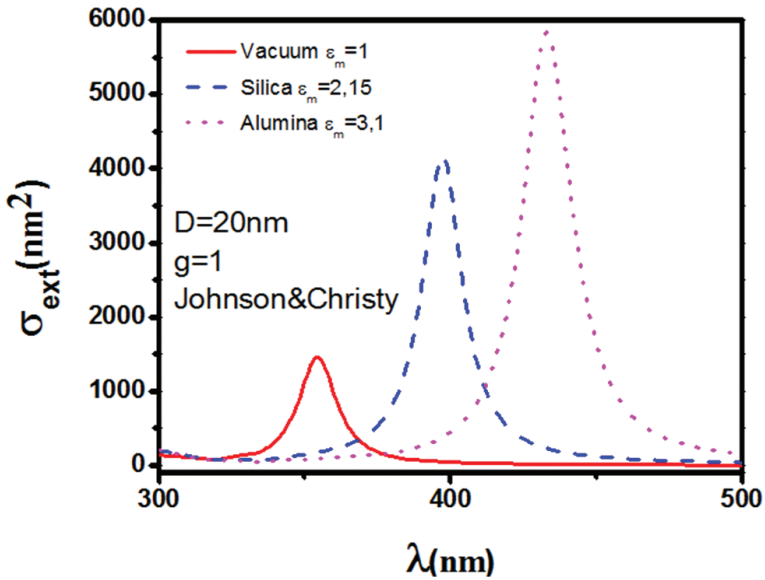


Figure 7. Extinction cross sections for a silver nanoparticle with a diameter of 20 nm calculated by the quasi-static approximation in different environments: Vacuum ($\epsilon_m = 1$), silica ($\epsilon_m = 2,15$) and alumina ($\epsilon_m = 3,1$).

extinction cross section of silver and gold nanoparticles in different environments was calculated (Figures 6 and 7). The dielectric constant used for the metallic nanoparticle was deduced from bulk metal by adding a surface contribution with $g = 1$ (Eq. 32). The redshift of the resonances is correlated to the increase of the dielectric constant of the external environment. It should be noted that this effect is more visible in the case of silver than in that of gold. For the latter, the immediate proximity of the threshold of interband transitions has the effect of attenuating and widening the surface plasmon resonance band when the spectral position is shifted toward the small wavelengths. Hence, an increase of ϵ_m has a less noticeable effect on gold than on silver.

8. Shape effect

So far, we have considered spherical nanoparticles. Experimentally, we are often led to study deformed particles which adopt ellipsoidal forms. On the basis of the notion of polarizability of particles, we establish here the general formulas of extinction cross sections for ellipsoids (semiaxes: a , b and c) in the quasi-static approximation (a , b and $c \ll \lambda$) and discuss the shape effect on the optical response.

By analogy with the case of the sphere, it is possible to show that the polarizability of an ellipsoid when an electric field is applied to it in one of the x , y or z directions is equal to [29]:

$$\alpha_{x,y,z} = \frac{4\pi}{3} abc \frac{\epsilon_1 - \epsilon_m}{3\epsilon_m + 3L_{x,y,z}(\epsilon_1 - \epsilon_m)} \quad (35)$$

To obtain this result, the Maxwell equations are solved in a system of ellipsoidal coordinates. The establishment of the boundary conditions at the interface between the particle and the external environment makes it possible to express the electrical potentials in each region and to identify the dipole responsible of the scattered field. The geometric factors $L_{x,y,z}$ are defined by:

$$\begin{cases} L_x = \frac{abc}{2} \int_0^\infty \frac{dt}{(t+a^2)^{3/2}(t+b^2)^{1/2}(t+c^2)^{1/2}} \\ L_y = \frac{abc}{2} \int_0^\infty \frac{dt}{(t+b^2)^{3/2}(t+a^2)^{1/2}(t+c^2)^{1/2}} \\ L_z = \frac{abc}{2} \int_0^\infty \frac{dt}{(t+c^2)^{3/2}(t+a^2)^{1/2}(t+b^2)^{1/2}} \end{cases} \quad (36)$$

$$L_x + L_y + L_z = 1 \quad (37)$$

By analogy with the problem of the sphere treated above, the cross sections can be expressed in the form:

$$\sigma_{ext} = 3k \operatorname{Im} \left\{ \alpha_x (\vec{e}_z' \cdot \vec{e}_x)^2 + \alpha_y (\vec{e}_z' \cdot \vec{e}_y)^2 + \alpha_z (\vec{e}_z' \cdot \vec{e}_z)^2 \right\} \quad (38)$$

$$\sigma_{diff} = \frac{3k^4}{2\pi} \left\{ |\alpha_x|^2 (\vec{e}_z' \cdot \vec{e}_x)^2 + |\alpha_y|^2 (\vec{e}_z' \cdot \vec{e}_y)^2 + |\alpha_z|^2 (\vec{e}_z' \cdot \vec{e}_z)^2 \right\} \quad (39)$$

$$\sigma_{abs} = \sigma_{ext} - \sigma_{diff} \cong \sigma_{ext} \quad (40)$$

An important case is that of an excitation by an electric field polarized collinearly with one of the principal axes of the ellipsoid. We can write:

$$\sigma_{ext}^{x,y,z} = \frac{2\pi\epsilon_m^{3/2} V}{L_{x,y,z}^2 \lambda} \frac{\epsilon_l}{\left(\epsilon_R + \frac{1-L_{x,y,z}}{L_{x,y,z}} \epsilon_m \right)^2 + (\epsilon_l)^2} \quad (41)$$

with $V = \frac{4}{3}\pi abc$ the volume of the ellipsoid. Depending on the direction of polarization $i = x, y$ or z , the resonance wavelength λ_{RPS}^i is determined by the relation:

$$L_i \epsilon_R (\lambda_{RPS}^i)^3 + (1 - L_i) \epsilon_m \cong 0 \quad (42)$$

The surface plasmon frequency for an ellipsoid:

$$\omega_{RPS}^{x,y,z} = \frac{\omega_p}{\sqrt{\operatorname{Re}\{\epsilon^{(IB)}(\omega_{RPS})\} + \frac{(1-L_{x,y,z})}{L_{x,y,z}} \epsilon_m}} \quad (43)$$

If the case of prolate ellipsoid ($a = c > b$), then $L_x = L_z$ and L_y depend only on its aspect ratio $\eta = \frac{a}{b}$. L_z is written as a function of the ellipticity e of the spheroids defined by: $e^2 = 1 - \eta^2$

$$L_y = \frac{(1 - e^2)}{e^2} \left[-1 + \frac{1}{2e} \ln \left(\frac{1 + e}{1 - e} \right) \right] \text{ and } L_{x,z} = \frac{1 - L_y}{2} \quad (44)$$

Figures 8 and 9 illustrate the evolution of SPR as a function of the shape of the ellipsoid in the case of gold and silver nanoparticles, respectively. The cross sections are calculated according to Eq. (41) for a prolate ellipsoid whose volume is equivalent to that of a 20-nm nanoparticle embedded in vacuum with $g = 1$. First, due to the anisotropy of the nanoparticle, there are two distinct modes for SPR on either side of SPR position of a sphere of the same volume. The difference between the two cases is more marked by decreasing the aspect ratio, as seen in

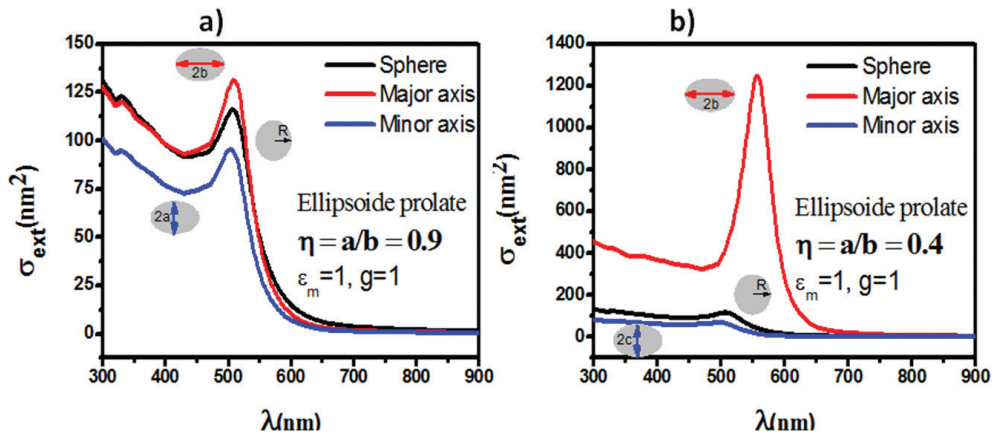


Figure 8. Extinction spectra calculated for a prolate gold nanoparticle for two aspect ratio values: (a) $\eta = 0.9$, (b) $\eta = 0.4$. The nanoparticle is placed in vacuum. The coefficient g of the surface term is taken to be equal to 1.

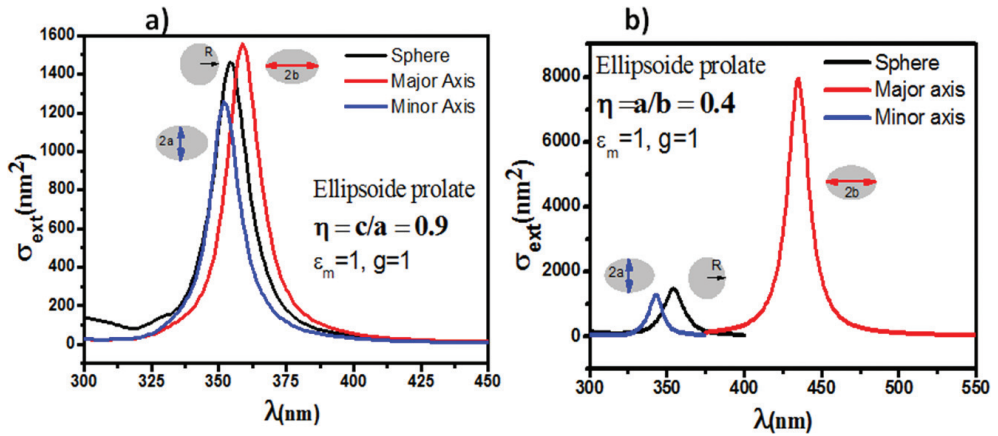


Figure 9. Extinction spectra calculated for a prolate silver nanoparticle for two aspect ratio values: (a) $\eta = 0.9$, (b) $\eta = 0.4$. The nanoparticle is placed in a vacuum. The coefficient g of the surface term is taken to be equal to 1.

Figures 8 and 9 for $\eta = 0.9$ and 0.4 . Indeed, the mode along the major axis gives a larger cross section because it is equivalent to a larger volume of material probed with respect to the sphere. In the case of gold and with the aspect ratio $\eta = 0.4$, it is found that the mode along the minor axis is wider than that along the major axis because the coupling with the interband transitions becomes stronger.

9. Mie theory

The quasi-static description developed previously is strictly valid only in the limit where $k \cong 0$. It gives a good approximation when $kR < 1$. For example, when $R \cong \lambda$, the applied electric field varies spatially on the volume of the particle. The distribution of surface charges does not necessarily have the dipole structure obtained for a uniform field, and multipolar contributions of higher orders are to be taken into account. We briefly present the formalism of the Mie theory which gives an exact general calculation of the optical response of a spherical particle of any diameter in a range of sizes where kR is no longer limited and may be greater than unit. In 1908, Gustav Mie developed a theory of the interaction of an electromagnetic wave with a homogeneous spherical metal nanoparticle based on a multipolar development of the electromagnetic field. This model describes the absorption spectrum of colloidal suspensions of gold particles in water [30]. We introduce the ratio M of the refractive indices of the nanoparticle and of the external dielectric medium and x the dimensionless size parameter:

$$M^2 = \frac{\varepsilon}{\varepsilon_m} = \left(\frac{n}{n_m} \right)^2 \quad \text{and} \quad x = kR = \frac{2\pi n_m R}{\lambda} \quad (45)$$

The important final result is that the extinction, scattering and absorption cross sections for a nanoparticle of diameter D are simply expressed as series [31, 32]:

$$\sigma_{ext} = \frac{2\pi}{k^2} \sum_{n=1}^{\infty} (2n+1) \text{Re}\{a_n + b_n\} \quad (46)$$

$$\sigma_{diff} = \frac{2\pi}{k^2} \sum_{n=1}^{\infty} (2n+1) (|a_n|^2 + |b_n|^2) \quad (47)$$

$$\sigma_{abs} = \sigma_{ext} - \sigma_{diff} \quad (48)$$

The coefficients a_n and b_n are defined by

$$\begin{cases} a_n = \frac{M\varphi_n(Mx)\varphi'_n(x) - \varphi_n(x)\varphi'_n(Mx)}{M\varphi_n(Mx)\zeta'_n(x) - \xi_n(x)\varphi'_n(Mx)} \\ b_n = \frac{\varphi_n(Mx)\varphi'_n(x) - M\varphi_n(x)\varphi'_n(Mx)}{\varphi_n(Mx)\zeta'_n(x) - M\xi_n(x)\varphi'_n(Mx)} \end{cases} \quad (49)$$

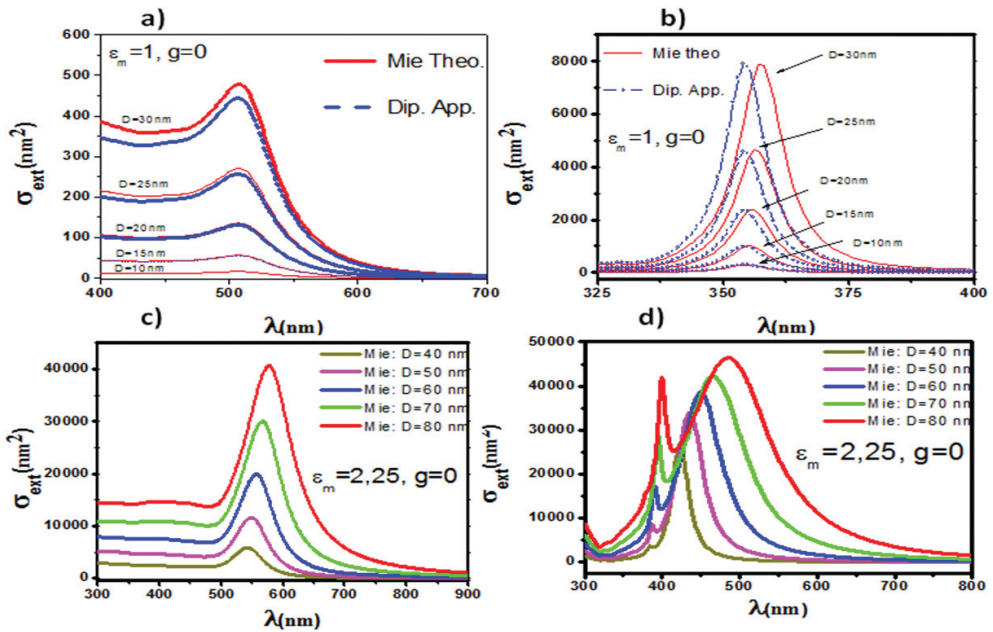


Figure 10. Extinction spectra calculated in the context of the Mie theory as a function of the size of nanoparticles in the case of gold (a) and (c) and silver (b) and (d). The spectra are compared with the calculations of the dipole approximation for sizes ranging from 10 to 30 nm in the case of gold (a) and silver (b).

where $\varphi_n(x)$ and $\xi_n(x)$ are the Riccati-Bessel functions of order n . The index n is the order of the multipole expansion. The quasi-static approximation is valid for diameters less than about 20 nm. In the case of gold, the resulting spectra show a dipolar peak which corresponds to the surface plasmon resonance at about 530–560 nm. Moreover, these spectra have a plateau below 500 nm which corresponds to the interband transitions. Finally, the signal falls to 0 and is practically zero from 750 nm (Figure 10a and c). In the case of silver, it can be seen that the increase of the size induces a widening and a redshift of the resonance due to the increasing influence of the multipolar terms (Figure 10b and d). This effect also exists for gold but is less clear due to the coupling of SPR with the interband transitions. The main peak in Figure 10d is attributed to the dipole character of the surface plasmon resonance, and the present appearance of second peak at higher energy is due to the quadrupolar contribution. The proximity of the interband transitions in gold (Figure 10c) explains that this contribution is not visible for a comparable nanoparticle size.

10. Optical response of several spherical particles: generalized Mie theory

Finally, we study a situation that can be encountered experimentally: the optical response of a group of close particles. This situation is illustrated in Figure 11. The incident field on a particle i is the sum of the applied field and the set of scattered fields by the other particles.

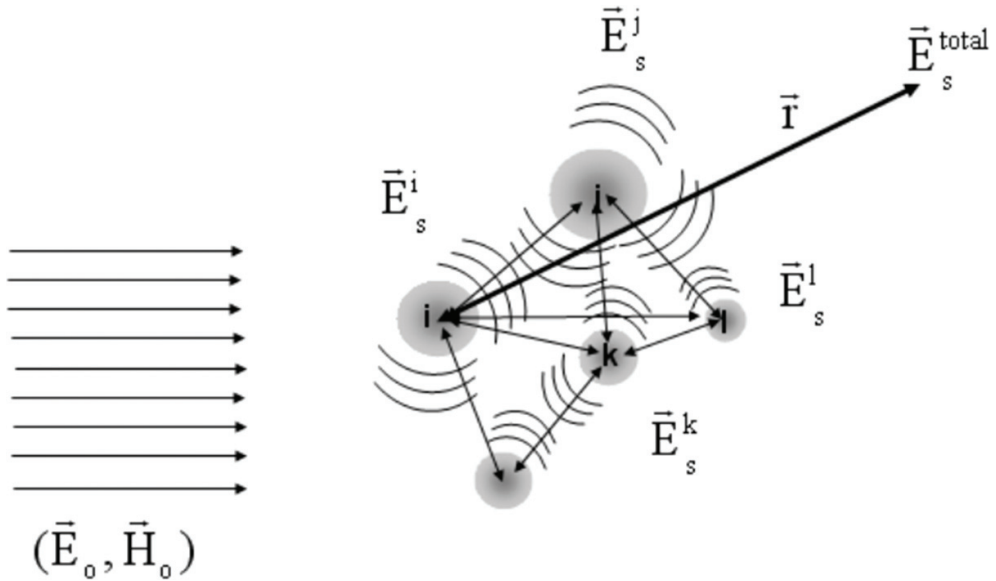


Figure 11. A scheme for exciting a group of spheres by an incident electromagnetic wave. The fields scattered by each particle can in turn excite neighboring particles.

$$\vec{E}_{inc}^i = \vec{E}_0 + \sum_{j=1, j \neq i}^N \vec{E}_s^j \quad (50)$$

The scattered field by a particle j depends on \vec{E}_0 and \vec{E}_{inc}^j . The optical response of the set will be obtained by solving this problem in a self-consistent way (coupled equations):

$$\vec{E}_{inc}^i = \vec{E}_0 + \sum_{j=1, j \neq i}^N f(\vec{E}_0, \vec{E}_{inc}^j) \quad (51)$$

In the case of spherical particles, this problem can be solved accurately but at the cost of a large numerical effort. The idea is to apply the results of the Mie theory developed previously since it allows to express the field scattered by a particle as a function of the incident field on this same particle. Nevertheless, for each of the particles considered, the theory requires to define a reference whose origin (center of the particle) and the orientation are fixed and linked to this particle [33–35]. **Figure 12** shows the extinction spectra of gold dimer nanoparticles as a function of the interparticle distance d calculated from the generalized Mie theory. The nanoparticles are supposed to be spherical, with a diameter $D = 100$ nm, and trapped in a medium with an effective index $n_m = 1.15$. The dielectric constant of gold is given by Johnson and Christy. For a distance $d = 10$ nm, the extinction spectra are presented for two orthogonal polarizations (**Figure 12**). When light is polarized perpendicular to the axis of the dimer (dotted spectrum in **Figure 12**), the extinction spectrum is similar to that of a single gold nanoparticle but twice more intense. The calculation shows that this extinction spectrum is in

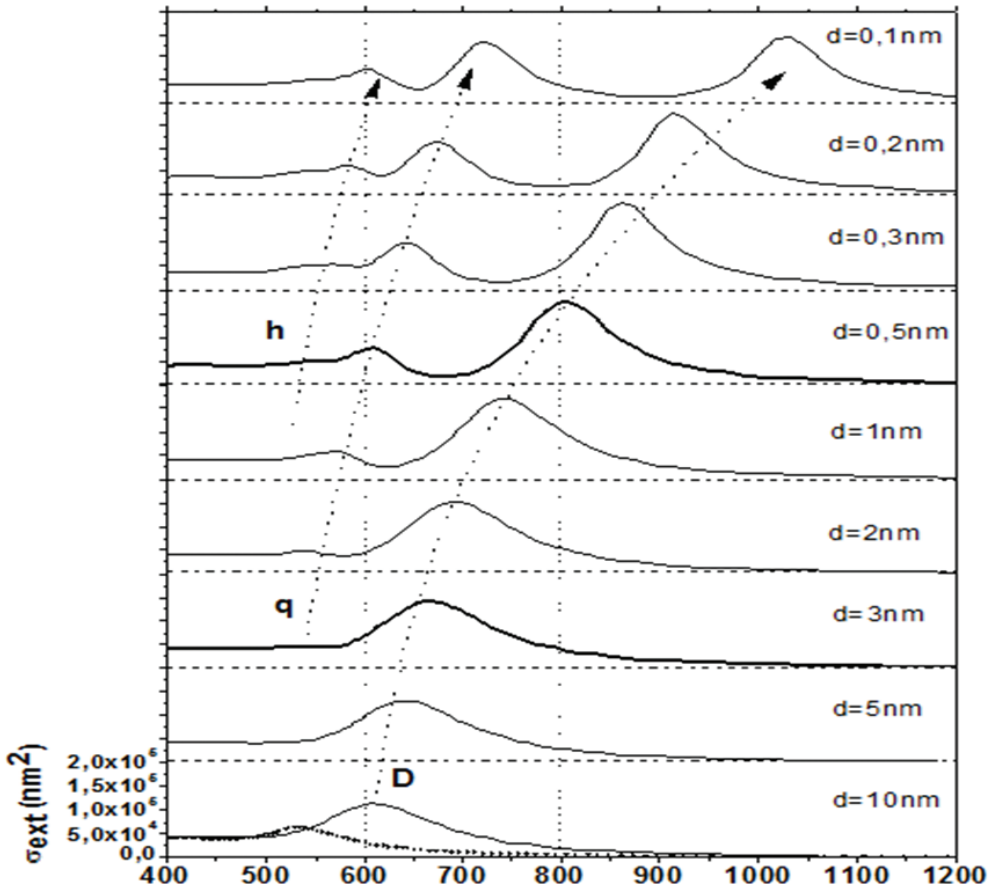


Figure 12. Extinction spectra (longitudinal excitation) of gold dimers ($R = 50 \text{ nm}$, $n_m = 1.15$) calculated by the generalized Mie theory as a function of the interparticle distance d . The dotted spectrum (for $d = 10 \text{ nm}$) is obtained for transverse excitation. To guide the eye, dotted arrows indicate the redshift of the dipolar (D), quadrupolar (q) and hexapolar (h) resonance. The spectra for $d = 0.5 \text{ nm}$ and $d = 3 \text{ nm}$ are highlighted.

fact independent of the distance d . For a direction of polarization of light along the axis of the dimer, it is found that the main resonance (peak D) shifts to red when d decreases. As the particles approach, peaks can be seen in the blue part of the spectrum (q and h). These peaks appear sequentially (q then h), grow and move toward red.

11. Conclusion

In this chapter, we demonstrated the capabilities of the Mie theory and quasi-static approximation to calculate the optical response of metallic nanoparticles. The quasi-static approximation is typically valid for nanoparticle diameter $D \leq \lambda/10$ (λ is the wavelength of the incident light). For other dimensions of size, we calculated the optical response in the framework of Mie

theory. We recalled the differences between extinction, absorption and scattering cross section of metallic nanoparticles. The spectrum of the extinction cross section present a resonance attributed to the collective oscillation of electrons in the conduction band: surface plasmon resonance (SPR). SPR spectral profile is very sensitive to the size, morphology and environment of the metallic nanoparticles. It is concluded that as the size of the spherical nanoparticle increases, the extinction magnitude increases whereas the spectral position of the surface plasmon resonance (SPR) is redshifted by using Mie theory. However, the peak position of SPR in quasi-static approximation is independent of size. We used the parameter g for confined nanoparticles to introduce the collision between electrons and the surface of nanoparticles. As the g factor increases, then there are more damping of oscillations. We concluded that the extinction cross-sectional magnitude is decreased and the width at half peak of SPR is increased. We investigated the effect of shape using dipolar approximation. We found that the surface plasmon resonance depends strongly on the polarization of the electromagnetic incident wave on the nanoparticle. As the aspect ratio decreases, the spectral position is shifted toward higher wavelength (when the light is polarized along major axis) and shifted toward smaller wavelength (when the light is polarized along minor axis). The mode along the long axis gives a larger extinction cross section because it is equivalent to a larger volume of material probed in relative to the sphere. We studied the extinction cross section of metallic nanoparticle embedded in different matrices. We remarked that the SPR is redshifted and accompanied by a large enhancement of its absorption cross section with increasing dielectric constant of the matrix. In the case of interacting systems, we have seen that the distance between nanoparticles is a crucial parameter. In the case of gold dimer nanoparticles, the smaller the interparticle distance, the more the dipolar resonance is redshifted with the appearance of higher order resonances.

Author details

Salem Marhaba

Address all correspondence to: s.marhaba@bau.edu.lb

Physics Department, Faculty of Science, Beirut Arab University, Lebanon

References

- [1] So DWC, Seshadri SR. Metal-island-film polarizer. *Journal of the Optical Society of America B*. 1997;**14**:2831
- [2] Lal U, Link S, Halas NJ. Nano-optics from sensing to waveguiding. *Nature Photonics*. 2007;**1**:641
- [3] Sharrouf M, Awad R, Marhaba S, Bakeer DE. Structural, optical and room temperature magnetic study of Mn-doped ZnO nanoparticles. *Nano*. 2016;**11**:1650042
- [4] Sharrouf M, Awad R, Roumié M, Marhaba S. Structural, optical and room temperature magnetic study of Mn₂O₃ nanoparticles. *Materials Sciences and Applications*. 2015;**5**:850

- [5] Stuart HR, Hall DG. Island size effects in nanoparticle-enhanced photodetector. *Applied Physics Letters*. 1998;**73**:3815
- [6] Akella A, Honda T, Liu AY, Hesselink L. Two photon holographic recording in aluminosilicate glass containing silver particles. *Optics Letters*. 1997;**22**:967
- [7] Ricard D, Roussignol P, Flytzanis C. Surface-mediated enhancement of optical phase conjugation in metal colloids. *Optics Letters*. 1985;**10**:511
- [8] Elvira D, Braive R, Beaudoin G, Sagnes I, Hugonin JP, Abram I, Philip IR, Lalanne P, Beveratos A. Broadband enhancement and inhibition of single quantum dot emission in plasmonic nano-cavities operating at telecommunications wavelengths. *Applied Physics Letters*. 2013;**103**:061113
- [9] Roumié M, Marhaba S, Awad R, Kork M, Hassan I, Mawassi R. Effect of Fe₂O₃ nano-oxide addition on the superconducting properties of the (Bi,Pb)-2223 phase. *Journal of Superconductivity and Novel Magnetism*. 2014;**27**:143
- [10] Basma H, Awad R, Roumie M, Isber S, Marhaba S, Abou Aly AI. Study of the irreversibility line of GdBa₂Cu₃O_{7- δ} added with nanosized ferrite CoFe₂O₄. *Journal of Superconductivity and Novel Magnetism*. 2016;**29**:179
- [11] Henry CR. Catalytic activity of supported nanometer-sized metal clusters. *Applied Surface Science*. 2000;**164**:252
- [12] Burchez M, Moronne M, Gin P, Weiss S, Alivisatos AP. Semi-conductors nanocrystals as fluorescent biological labels. *Science*. 1998;**281**:2013
- [13] Faraday M. Experimental relations of gold (and other metals) to light. *Royal Society of London*. 1857;**147**:145-181
- [14] Maxwell Garnett JC. Colours in metal glasses and in metallic films. *Philosophical transactions of the Royal Society of London, Serie B*. 1904;**203**:385
- [15] Marhaba S. Gold nanoparticle arrays spectroscopy: Observation of electrostatic and radiative dipole interactions. *S. Nano*. 2015;**10**:1550007
- [16] Baida H, Billaud P, Marhaba S, Christofilos D, Cottancin E, Crut A, Lermé J, Maioli P, Pellarin M, Broyer M, Del Fatti N, Vallée F, Sánchez-Iglesias A, Pastoriza-Santos I, Liz-Marzán LM. Quantitative size dependence of the surface plasmon resonance damping in single Ag@SiO₂ nanoparticles. *Nano-Letters*. 2009;**9**:3463–3469
- [17] Billaud P, Marhaba S, Cottancin E, Arnaud L, Bachelier G, Bonnet C, Del Fatti N, Lermé J, Vallée F, Vialle JL, Broyer M, Pellarin M. Correlation between the extinction spectrum of a single metal nanoparticle and its electron microscopy image. *Journal of Physical Chemistry C*. 2008;**112**:978-982
- [18] Pines D. A collective description of electron interactions. IV. Electron interactions in metals. *Physical Review*. 1953;**92**(3):626
- [19] Kittel C. *Physique de l'état solide*, 7ème édition. Dunod, Paris; 1998

- [20] Ashcroft NW, ND Mermin. Solid State Physics. International Edition, Saunders College, Philadelphia; 1976
- [21] Johnson PB, Christy RW. Optical constants of the noble metals. *Physical Review B*. 1972; **6**(12):4370
- [22] Palik ED. Handbook of optical constants of solids. London: Academic Press Inc; 1985
- [23] Berthier S. *Optique des milieux composites*. Paris: Polytechnica; 1993
- [24] Kreibig U, Vollmer M. *Optical properties of Metal Clusters*. Berlin: Springer Verlag; 1995
- [25] Kreibig U, Genzel L. Optical absorption of small metallic particles. *Surface Science*. 1985; **156**:678
- [26] Billaud P. *Propriétés optiques de nanoparticules uniques de métaux nobles*. Thèse de Doctorat, Université Lyon 1; 2006
- [27] Del Fatti N. *Dynamique électronique femtoseconde dans les systèmes métalliques massifs et confinés*. Thèse de Doctorat, Université Bordeaux 1; 1999
- [28] Muskens OL, Bachelier G, Del Fatti N, Vallée F, Brioude A, Jiang X, Pileni MP. Quantitative absorption spectroscopy of a single gold nanorod. *Journal of Physical Chemistry C*. 2008; **112**(24):8917
- [29] Bohren CF, Huffman DP. *Absorption and scattering of light by small particles*. New York: Wiley; 1983
- [30] Mie GG. Beiträge zur Optik trüber Medien, speziell kolloidaler Metallösungen. *Annals of Physics*. 1908; **25**(3):377
- [31] Lermé J, Bonnet C, Broyer M, Cottancin E, Marhaba S, Pellarin M. Optical response of metal or dielectric nano-objects in strongly convergent light beams. *Physical Review B*. 2008; **77**:245406
- [32] Lermé J, Bachelier G, Billaud P, Bonnet C, Broyer M, Cottancin E, Marhaba S, Pellarin M. Optical response of a single spherical particle in a tightly focused light beam: Application to the spatial modulation spectroscopy technique. *Journal of the Optical Society of America A*. 2008; **25**:493-514
- [33] Gérardy JM, Ausloos M. Absorption spectrum of clusters of spheres from the general solution of Maxwell's equations. The long-wavelength limit. *Physical Review B*. 1980; **22**(10):4950
- [34] Gérardy JM, Ausloos M. Absorption spectrum of clusters of spheres from the general solution of Maxwell's equations. II. Optical properties of aggregated metal spheres. *Physical Review B*. 2004; **25**(6):4950
- [35] Marhaba S, Bachelier G, Bonnet C, Broyer M, Cottancin E, Grillet N, Lermé J, Vialle JL, Pellarin M. Surface plasmon resonance of single gold nanoparticle pairs near the conductive contact limit. *Journal of Physical Chemistry C*. 2009; **113**:4349-4356